Traveling excitable waves successively generated in a nonlinear proliferation system

Kenta Odagiri and Kazuo Takatsuka
Department of Basic Science, Graduate School of Arts and Sciences, The University of Tokyo, 153-8902 Tokyo, Japan
(Received 26 November 2008; revised manuscript received 18 March 2009; published 18 May 2009)

We study the dynamics of spatiotemporal pattern formation in a nonlinear proliferation system (e.g., cell division supported on a field of nutrition), in which the mechanism of activation and its self-suppression is simultaneously implemented. This dynamical model has been numerically realized with coupled cellular automata (CA), and various long-standing spatiotemporal patterns have been observed. Among others, a successive generation of traveling waves by implanting a spot of cells onto the field consisting of nutrition and activator is particularly interesting. This takes place despite the fact that the present reaction network has a stable fixed point and therefore autonomous temporal oscillatory does not exist in the mean field. Indeed, the reaction-diffusion equation method (RD) applied to this network reproduces only a single excitable wave and soon falls into a steady state (a fixed point) without the following propagating waves. This system, having a stable fixed point, is an excitable system of different kind from the FitzHugh-Nagumo model in that it can generate a pulse propagating outwards by adding only a single cell onto it from outside the system. The present excitation upon dropping a cell is amplified to macroscopic level by a hidden dynamics of oscillation between the activation and its self-suppression. A pulse thus generated is propagated in space time with the help of diffusion. Through a precise comparison between CA and RD, it is found that a very small amount of residue of the cells and activators, which are left unburned in the stochastic treatment of reactions by the CA, becomes a seed to excite the system and generate the next pulse wave. This newly born wave can leave another seed of reaction in the field after its propagation. Based on this analysis, we account for the appearance of other patterns observed. A possible control of these patterns by varying the spatial distribution of initial concentration of the relevant agents such as the activator is also discussed.

DOI: 10.1103/PhysRevE.79.056219 PACS number(s): 82.40.Ck, 05.40.−a, 05.65.+b, 02.50.Ey

I. INTRODUCTION

Nonlinear growth in multiple agent systems such as those in autocatalytic reactions is often associated with pattern formation ubiquitously, ranging from the atomic scale phenomena [1] to the morphology of living bodies [2]. It is quite interesting to explore how those diverse patterns are generally ruled. Among others, in this paper, we study successive spatiotemporal evolution of traveling waves (autonomous successive pulse generation) generated in excitable media due to nonlinear proliferation dynamics.

It is widely recognized that there are at least two mechanisms that can generate pulse wave(s) in chemical and/or biological systems [3–7]. One is the so-called oscillatory system of "reaction" network (not necessarily chemical reactions), which has a temporal oscillation under stirred condition (in a mean field). In a static experimental situation, this system propagates self-sustained pulse waves forming a pattern such as the concentric ring pattern in space time. The initial pulse is caused by a pace-maker or the presence of an initial phase shift and the successive pulses are propagated outward with the help of diffusion. The most well-known example of such a system is the Belousov-Zhabotinskii (BZ) reaction under appropriate experimental conditions [8]. A mathematical model reduced from the BZ reaction, Oregonator, has been established and the mechanism of the temporally oscillatory reaction in a mean field is now well understood [9,10]. The BZ reaction also shows various spatiotemporal patterns such as spiral patterns and target patterns depending on the conditions imposed and it is known that the reaction-diffusion equation (RD) method reproduces such a dynamical pattern quite well [11,12].

The other important mechanism of generating a pulse is observed in the so-called excitable system. An excitable system sits on a stable fixed point and is static. However, when applied an external perturbation or noise of an amplitude larger than a threshold value, the system can undergo excitation taking a circuit path in state space before returning to the fixed point. To generate pulses successively, continuous noise should be applied. Furthermore, Pikovsky and Kurths [13,14] found the existence of an intensity of noise that maximizes the coherence among thus generated pulses. The FitzHugh-Nagumo (FN) equation, a mathematical model of transmittance of excitement through nerve axon under an appropriate set of system parameters, is a well-known example of the excitable system.

In the present paper, we report our finding of a system that exhibits a self-sustained (i.e., not driven by external noise) generation of successive traveling waves but its mean-field counterpart is not oscillatory in contrast to the BZ reaction. Indeed, the solution of its reaction network falls into a fixed point if diffusion is not present. Therefore the last half of the present paper is devoted to clarification of the mechanism of these successive traveling waves. We also investigate how to control the appearance of such dynamical patterns.

Diffusion and noise (or fluctuation) [15] are the key quantities in the study of pattern formation. The reaction diffusion equation approach with or without stochastic noise, which are often based on a mean-field description such as the rate equations in chemical reaction systems, and the cellular automaton (CA) [16] are among the most widely used methods in pattern formation dynamics. They have their own virtues. However, it sometimes happens that these two methods give different solutions, namely, different pattern formation to the

same problem. We have reported and analyzed the origin of their difference in a very simple model study of static pattern formation of bacteria colony [represented in Eqs. (1a) and (1b)] [17]. It turns out that the natural treatment of noise and its induced symmetry breaking in the CA algorithm are all favorable to generation of wide variety of patterns. Here in treating the dynamics of Eqs. (2a)–(2e), another dramatic difference between CA and RD is found, which should give a critical clue for the mechanism of the successive traveling waves.

The paper is organized as follows. In Sec. II, we introduce our model system of nonlinear proliferation system, which includes the activation process for proliferation and its self-suppression. Various dynamical patterns emerging in the CA simulation of this system are exhibited. We also show an interesting example suggesting a possible control of pattern formation. Section III is devoted to phenomenological analyses on how the basic spatiotemporal patterns have emerged, particularly on the mechanism of the wave propagation in the early stage. In Sec. IV we attempt to extract more generic mechanism of the self-sustained generation of successive traveling waves by identifying the present system to be an excitable system of a different kind from the FitzHugh-Nagumo system. To clarify the mechanism proposed, we compare the CA with the relevant RD equations with and without noises. This paper concludes in Sec. V with some remarks.

II. CELLULAR AUTOMATA STUDY ON A PROLIFERATION SYSTEM INVOLVING THE PROCESSES OF ACTIVATION AND INHIBITION

A. Dynamical system studied

We first describe our system of autocatalytic reaction. We begin with a very basic system consisting of a proliferating agent, say a cell, X and nutrition N, whose dynamics is

$$X + N \rightarrow 2X, \tag{1a}$$

$$X \rightarrow P_1. \tag{1b}$$

X is transformed to an inactive body P_1 subject to a given probability if it misses N. Complicated patterns such as the so-called viscous finger have been found to emerge from such a very simple system [17]. To seek further for spatiotemporal patterns, we add a pair of mutually antagonistic elements, activator (A) and inhibitor (I). The actions balancing between these elements can potentially give birth to a large fluctuation in dynamics, which is crucial to the successive wave generation as observed below.

After surveying many different reaction networks, we have found a system that gives particularly interesting phenomena. It is the following network: system PIA (proliferation system with inhibition and activation),

$$X + A \rightleftharpoons X^*, \tag{2a}$$

$$X^* + N \rightarrow 2X + 2A, \tag{2b}$$

$$X \rightarrow P_1 + \alpha I, \tag{2c}$$

$$A + I \rightarrow N, \tag{2d}$$

$$I \rightarrow P_2. \tag{2e}$$

It is not difficult to interpret the above sequence of dynamics: a cell (X) can be doubled by consuming nutrition (N) [Eq. (2b)], only after it is activated (or energized) by the activator (A) with X^* being an activated intermediate of X [Eq. (2a)]. The activator A is also doubled in this cell division process. When X dies for starvation [Eq. (2c)], it emits an inhibiting agent (I), which can annihilate the activator A [Eq. (2d)]. The inhibitor itself is to be eventually extinguished if it does not encounter A [Eq. (2e)].

Some notes about this model would be in order. (i) This network represents a set of procedures to drive a general nonlinear proliferation dynamics, although we would not specify a realistic system from which this model can be extracted. It should be understood therefore that these equations do not necessarily obey the mass action law based on the conservation of mass, and therefore the coefficients in the equations do not indicate the stoichiometry of chemical reactions. On the other hand, the number of cells, for instance, is not simply proportional to its weight, depending on the species and age. Furthermore, some of the environmental quantities such as the extent of sunshine are not explicitly considered in the above dynamics. For instance, we may reformulate Eq. (2c) as $X+S_1 \rightarrow P_1+\alpha I$, where S_1 is an external source of, say, energy, which nevertheless does not modify the results presented below. (ii) We note that the inhibitor here is designed to suppress the activation process [Eq. (2d)] but not reducing (killing) the cells directly. We have examined such a system, which includes $X+I \rightarrow 2N$ in place of the process of [Eq. (2d)], and found nothing particularly exciting. (iii) We occasionally call X and N cell and nutrition, respectively, in the following text as though we were mimicking a biological system. However, this does not have to be the case, and these agents may be regarded as general elements consisting of a group or community. Finally, in the present CA, every element is counted as an integer number.

B. Coupled cellular automata used

The coupled cellular automata used in this paper is essentially the same as that we have developed and applied in the previous paper [17], and the reader may want to skip to the next subsection. The methodological details are referred to that paper and Ref. [18], and we here outline only the part particularly relevant to the present work. We describe technical details and algorithms actually applied in the Appendix. For the discussion for coupled CA, see also [19].

The CA dynamics applied to the present system, Eqs. (2a)–(2e), consists of five CA's fields, and each CA field represents the spatiotemporal distribution of the number of particles of each component. With these fields, we run the following three procedures: (1) diffusion process on each field, (2) reaction process through the communication of each field, and (3) the coupling between reactions and diffusion. The diffusion on each CA is allowed to be evolved in

time independently from other CA's, whereas the reactions are treated as interactions between the particles on different CA's. The ratio of time steps of these automata should be determined so as to represent the physical constants predetermined such as those for the reaction rates and diffusions. Each CA field realizes cellular dynamics on two-dimensional triangular lattice coordinates, in which any single node has six nearest-neighbor nodes, except for those on the boundary.

These diffusive motions are treated as a random walk in each CA field. Each particle is allowed to move to one of its nearest-neighbor nodes or remains at the same node. Let p_i be a probability for a particle of the component i to stay at the same node $(0 \leq p_i \leq 1)$. Since particles can diffuse in an isotropic manner, the probability of moving to one of the nearest-neighbor nodes is $(1-p_i)/6$ in the triangular coordinate system. Running a random number in $[0,1)$, we determine the position to which a particle should move.

The reaction process is treated as an interaction between the relevant independent CA's, which are responsible for different agents. We regard each reaction as a stochastic process and set a predetermined probability for particles to react in a unit time Δt_R (we define Δt_R later).

The diffusion processes for different components on the individual CA's run independently with their own time intervals. They are periodically forced to couple with each other for the reactions in a certain time interval. These timings are fixed by the following relations. Suppose that Δt_{D_i} is a unit time length for the diffusion process of a component i. Also, let Δt_R be the unit time interval for the communication of each CA's to be made to take account of the reactions. Then the relative length for these timings are numerically fixed by predetermining the ratio (diffusion frequency) $\tau_i = \Delta t_R / \Delta t_{D_i}$. The diffusion frequency τ_i is correlated with the diffusion constant D_i of the component i in the present stochastic model such that [17]

$$D_i = \frac{(1-p_i)\tau_i}{4}, \tag{3}$$

where $1-p_i$ is the mobility of particles given above in the description of diffusion process.

C. Patterns varying with the initial concentration of activator and nutrition

We here show that the model [Eqs. (2a)–(2e)] can generate various spatiotemporal dynamics of pattern formations with the CA method. For these to happen, an appropriate value of α in Eq. (2c) should be predetermined so as to satisfy $\alpha > 1$. If $\alpha < 1$, the number of potentially produced particles of I from a single X is less than 1. Furthermore, an I particle can produce at most a single N particle in the inhibition reaction [Eq. (2d)], so that the number of potentially produced N particles is less than 1 under a single occurrence of the proliferation of X. This implies that the total amount of N keeps decreasing and N is eventually exhausted, resulting in the termination of the entire reactions. On the other hand, if α is too large, too much I is produced in reaction (2d), and consequently the spatiotemporal patterns are not generated because of the too strong inhibitory effect.

TABLE I. System parameters chosen for the cellular automata.

X_0	50	p_X	1/7	τ_X	1
N_0	[a]	p_N	1/7	τ_N	1
I_0	0	p_I	1/7	τ_I	1
A_0	[b]	p_A	1/7	τ_A	1
X_0^*	0	p_{X^*}	1/7	τ_{X^*}	1
r_1 [c]	0.90	r_2 [c]	0.90	r_3 [c]	0.15
r_4 [c]	0.90	r_5 [c]	0.25	r_1^* [d]	0.05

[a]To be varied as controlling parameters.
[b]To be varied as controlling parameters.
[c]r_1, r_2, r_3, r_4 and r_5: reaction probability in Eqs. (2a)–(2e), respectively.
[d]Reaction probability of the reverse process in Eq. (2a).

After surveying these possibilities numerically, we hence set $\alpha = 3$ in this paper.

We now show some typical spatiotemporal patterns which are generated in system PIA. As an initial condition, a small droplet consisting of X is placed at the center of the field, and N and A are uniformly distributed over the system. No I is initially prepared. The system parameters used are summarized in Table I and the periodic boundary condition has been imposed. The basic pattern is concentric ring pattern (CRP), which is born under the initial parameters $(N_0, A_0) = (10, 5)$ as shown in Fig. 1. The excitable waves generated from two spiral cores near the center of the system form concentric rings. In this case, the densities of the individual components oscillate "periodically" at a point marked with ○ in panel (a) of Fig. 1 as shown in panel (b).

In addition to the above standard CRP, we observe a variety of spatiotemporal and stationary patterns in this system by changing the initial condition (N_0, A_0). They are roughly classified as follows (see Fig. 2): (i) CRP, shown as above [Figs. 1 and 2(b)]. (ii) Random ring pattern (RRP), which is generated in various points with random time intervals. This pattern formation lasts for a long time [Fig. 2(a)]. (iii) Turbulent wave pattern (TWP), which consists of numerous excitable waves generated from the spiral cores at various points over the entire field [Fig. 2(d)]. (iv) Spatially homogeneous distribution (SHD), in which only X, X^* and A are

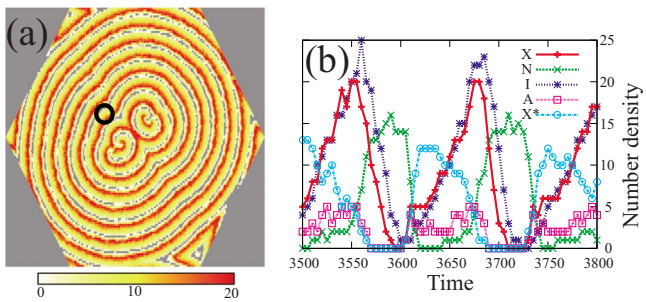

FIG. 1. (Color online) (a) Snapshot of the X distribution at $t = 3500$ in a concentric ring pattern. The color bar indicates that the darker (red) part contains the more X particles. (b) Time evolution of the individual components monitored at a point marked with ○ in panel (a).

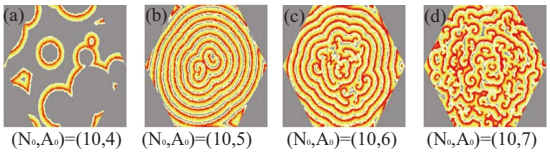

FIG. 2. (Color online) Snapshots of the X distribution for different initial number density of $A(A_0)$. N_0 is fixed at 10 throughout. (a) RRP (A_0=4), (b) CRP (A_0=5), (c) CRP+TWP (A_0=6), and (d) TWP (A_0=7). All the figures display the pattern at t=5000.

uniformly distributed (not shown). (v) Vanished pattern (VP), in which the excitable wave is generated only once from the initial pointlike area of X and then extinguished leaving only N behind (not shown).

The phase diagram of these patterns on a surface of (N_0, A_0) is given in Fig. 3. The generating mechanism of each pattern is described in the next section. Incidentally, our numerical calculations have revealed that the system PIA can also generate both the various Turing patterns and the self-replicating pattern subject to the condition that N and I diffuse faster than the other components. However, this aspect is not in the main scope of this paper.

D. Possible control of pattern formation

Through the above numerical studies, it turns out that the ratio of the amount of A_0 to that of $N_0(A_0/N_0)$ can be regarded as a good parameter to specify the patterns. This suggests that an interesting pattern can be given by the spatially inhomogeneous distribution of these components. For instance, the pattern formation observed in Fig. 2 suggests that a spatial gradient of the concentration of A_0 with a uniform distribution of N_0 would make a new pattern. Figure 4 shows such an example. Figure 4(d) exhibits a gradient of A_0, which has the smaller value in the upper part of the field. The resultant pattern shows the coexistence of the CRP and TWP in the upper and lower half areas, respectively. These wave patterns are dynamically propagated, but the regions they individually cover do not change much for a long time. This

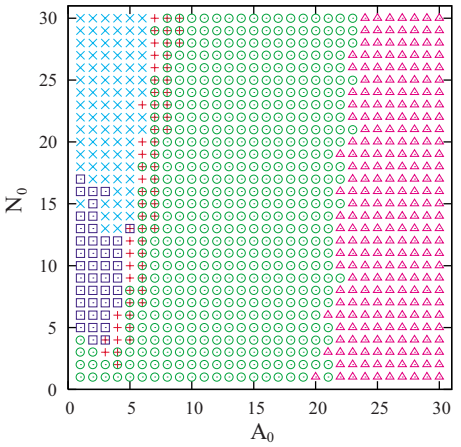

FIG. 3. (Color online) Phase diagram with respect to A_0 and N_0. The symbols represent (+) CRP, (□) RRP, (○) TWP, (△) SHD, and (×) VP.

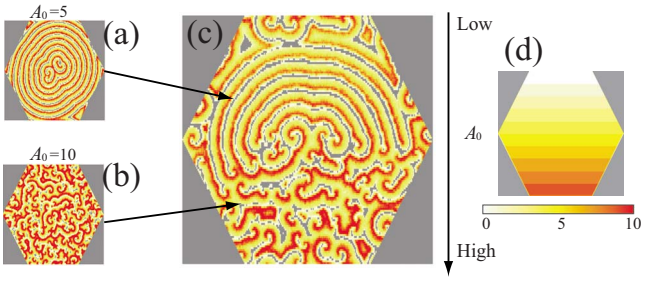

FIG. 4. (Color online) (c) Snapshot at t=5000 of the X distribution in the system that has a gradient in the initial distribution of A_0 as shown in the panel (d). CRP (a) and TWP (b) appear in the upper and lower half spaces, respectively. Two domains maintain a stable balance for a long time.

is possible because both patterns happen to have almost the same oscillation frequency (this has been verified with the Fourier analysis).

It is thus clarified that the spatial distribution of A_0 may be utilized as a control parameter to determine the ultimate patterns. This aspect deserves further study. Indeed, the present study has been partially stimulated in a qualitative fashion by the remarkable discovery of Asashima *et al.* [20] that the initial gradient of activins (a morphogen) in the process of cell differentiation after fertilization controls which organs are to be formed in a biological system.

III. PHENOMENOLOGICAL MECHANISM OF PATTERN FORMATION IN CA DYNAMICS

We first analyze the detailed mechanism for the formation of the patterns from phenomenological view point. The more abstract and generic mechanism extracted from phenomenology is discussed in the next section in more general context.

A. Mechanism of the concentric ring pattern

We here focus on spatiotemporal dynamics of the CRP as a basic pattern emerging in system PIA and numerically clarify the basic mechanism of temporal oscillation and successive wave propagation in the early stage.

1. Implicit mechanism of temporal oscillation

We first describe the detailed mechanism of temporal oscillatory behavior of each component at a point [see Fig. 1(b)] due to successive wave propagation. We first note that Eqs. (2a)–(2e) can be roughly divided into two parts from the viewpoint of functioning: subprocess (P)

$$X + A \rightleftharpoons X^*, \tag{4a}$$

$$X^* + N \rightarrow 2X + 2A, \tag{4b}$$

subprocess (S)

$$X \rightarrow P_1 + 3I, \tag{5a}$$

$$A + I \rightarrow N, \tag{5b}$$

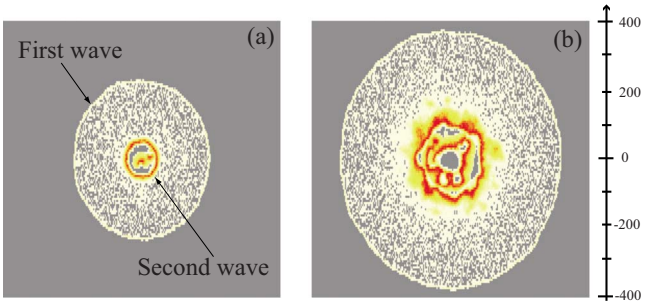

FIG. 5. (Color online) Birth and propagation of the waves in the early stage of spatiotemporal pattern formation in system PIA. (a) The wave fronts of the first and second waves are clearly observed in the concentration of X. Even the seed of the third wave is already seen (t=400). (b) Break of the second wave at a later time (t=650), which is closely followed by the mature wave.

$$I \rightarrow P_2. \tag{5c}$$

In the propagation process (P), the element X increases consuming N, as long as the activator A is available. On the other hand, a large amount of X produced in (P) triggers the suppressing process (S) and produces the inhibitor I, which reduces A to N. This reduction of A in turn suppresses the activation process of (P), resulting in fewer production of X. Then, the fewer supply of X from (P) makes the process of (S) slower with some time delay, which reduces the amount of I concomitantly. However, after the subprocess (S) "terminates," an abundance of N's are left behind, which may be utilized if the next burst of subprocess (P) can resume. (As will be shown later, the actual wave-propagation dynamics requires a little more precise analysis.)

2. Successive waves propagation in the early stage

The most characteristic aspect in the formation of spatiotemporal pattern in the model [Eqs. (2a)–(2e)] is found in its very early stage. As described below in great detail, we observe the successive propagation of discrete concentric wave fronts blowing outward. Below we track the sequential propagation of these wave fronts.

a. Two-stage wave dynamics. Several waves are born sequentially at the point where X is initially implanted and then each is propagated forming a clear wave front individually. See Fig. 5(a), where the wave fronts of the first and the second waves are clearly observed.

The natures of the first and second waves are totally different. The first wave has a low concentration of X and travels fast, leaving a high concentration of X^* behind in the field. On the other hand, the second wave front contains a high concentration of X and travels very slowly at first. However, the clear circular wave front of the second wave breaks suddenly at some time later [Fig. 5(b)], and its shape begins to fluctuate violently looking like flame. Incidentally, the vertical axis right to panel (b) of Fig. 5 represents the radial coordinate of the CA field, which is to be denoted as r in what follows.

b. First wave. Figure 6 shows a snapshot at t=400 of the spatial concentration (in the radial direction) of the individual components nearby the first wave front. The dynamics of the individual components is summarized as follows: X makes a pulse at the wave front by sudden increase from zero and decrease to a small amount, that is, only a little X is left behind within the wave. On the other hand, X^* forms a kink by rapidly increasing from zero to a large amount. Compensating this sudden increase, N makes an antikink by changing from an almost uniform distribution of the initial high concentration to a very small value. Thus N has been exhausted *almost completely*. The concentration of A is a little higher after the passage of the wave front (recall that A was uniformly distributed in the initial condition). No I is observed in this stage.

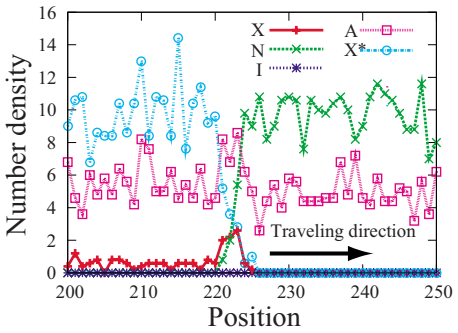

FIG. 6. (Color online) Spatial distributions of the concentration of the individual components near the wave front of the first pulse in the radial direction at t=400.

Summarizing these dynamical changes of the concentrations, we can readily conclude that this first wave is driven almost only by subprocess (P), Eqs. (4a) and (4b). The total amount of X increases exponentially with a full use of the two steps of Eqs. (4a) and (4b). However, the exponential shortage of N soon terminates the process $X^*+N \rightarrow 2X+2A$ and the process $X+A \rightarrow X^*$ consumes much of X leaving X^* behind. Eventually this step is also terminated by the shortage of X. Thus it turns out that the first wave effectively changes the CA field so that $N(+A) \rightarrow X^*(+A)$. With this modification, the field becomes ready to be followed by the second wave.

Such modification of the field by the first wave as above is necessary for the second wave to be generated and propagated. To confirm this view, we have examined dynamics arising from the different set of initial conditions having $(N_0, X_0^*)=(0,10)$ in place of $(N_0, X_0^*)=(10,0)$. Under this condition, essentially the same wave as the second wave, which will be described below, has been generated at the outset without the generation of a guiding wave like the first wave.

c. Second wave. After the passage of the first wave, the second wave is born in the field that is already filled with much X^* and a little N. Figure 7 shows a snapshot of the spatial distributions of the individual components at t=400, which has the pulses of X involved in the first wave at $r \sim 220$ and the second one at $r \sim 50$. In the area of the second wave, we observe the following: (i) X forms a much higher pulse than that of the first wave, (ii) I also makes a pulse

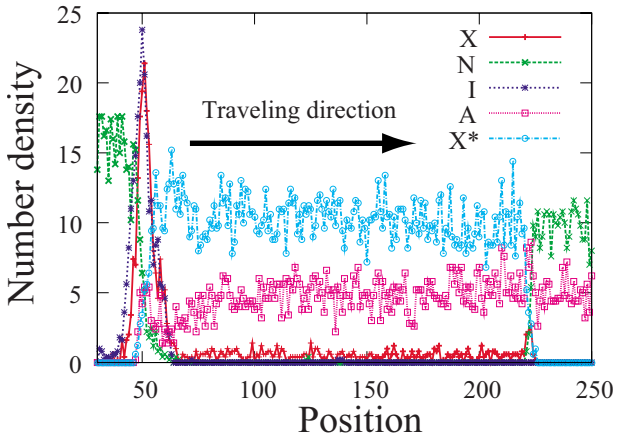

FIG. 7. (Color online) Spatial distributions of the concentration of the individual components near the wave fronts of the first wave ($r \sim 220$) and the second wave ($r \sim 50$) at $t=400$.

whose phase comes a little later than that of X, (iii) both X^* and A are exhausted almost completely, and (iv) N increases dramatically and recovers to a higher level than the initial one (recall that A was also prepared in the initial condition).

Due to the passage of the first wave, X and N are mostly exhausted. But, X is consumed not only in $X+A \rightleftharpoons X^*$, but also in $X \rightarrow P_1+3I$, which produces significant amount of the inhibitor I. I thus produced consumes A in $A+I \rightarrow N$ and thereby represses the activation process Eq. (2a) and at the same time reproduces N. N thus produced in turn burns X^*, which has already filled the field after the first wave, in the process $X^*+N \rightarrow 2X+2A$. Thus it turns out that $X^*+N \rightarrow 2X+2A$ plays an important role in subprocess (S) too. Therefore subprocess (S) should be modified so as to include this reaction within it; subprocess (S′)

$$X^* + N \rightarrow 2X + 2A, \tag{6a}$$

$$X \rightarrow P_1 + 3I, \tag{6b}$$

$$A + I \rightarrow N, \tag{6c}$$

$$I \rightarrow P_2. \tag{6d}$$

After A has been almost completely consumed up as shown in Fig. 7, this subprocess (S′) effectively stops and the field is mostly filled with N.

d. Merge of the second and third waves. Then the third wave follows. Figure 8 displays what happens to the second and third waves sequentially. Panel (a): the third wave, which travels fast, follows right behind the slowly moving second wave ($r \sim 60$). Panels (b) and (c): then these waves contact each other. The fourth wave appears already behind them. Panel (d): these two waves finally merge. At the same time, the second wave becomes broad in the forward direction and its shape begins to be deformed, reflecting that this part ($r=100 \sim 130$) in the front end of the second wave becomes activated because of the increase of I that is diffusing into this region. Panel (e): the merged wave becomes even broader. Panel (f): X in this broad region rapidly increases by the proliferation reactions [subprocess (P)], and the peak becomes bimodal again. Panel (g): the inner peak ($r \sim 160$) of the bimodal peaks decays, because the inhibiting process rapidly proceeds because of the excess I left behind. Panel (h): finally, the pulse originally arising from the second and third waves becomes a single peak again. It turns out that the shape of this wave is now similar to that in panel (d). The similar deformation of the wave experiencing from panel (d) through (h) is repeated. By this merge of the second and third waves, the field behind the merged wave is filled mostly with N again [see panel (h)].

It seems in a macroscopic scale as though the CA field is occupied exclusively by N after the propagation of the merged waves and therefore there was no seed for the following core to be generated. The reality is, however, that a small amount of X and A (or X^*) can be left behind because of the stochastic fluctuation realized by the CA dynamics. These surviving particles of X and A (or X^*) can ignite the reaction process of subprocess (P), since the abundant N coexisting at the same place can support the reaction and help the formation of a next core. Figure 9 evidences this situation clearly.

e. Mature waves. Following the second wave, new waves are generated from the cores which are in turn formed from the residual particles (rump) of X and A (or X^*) after passing of the second wave (see Fig. 9). We collectively refer to these waves as the mature wave in what follows. Any mature wave propagates with almost a steady shape outwards with almost the same speed (see Fig. 10). A precise look at the mature wave of X in this figure shows that it has a small bump in the front part of the wave ($r \sim 175$). This small shoulder (bump) should work like the first wave. However, the essential difference is that the "second wave" (the main part of the mature wave) follows right after the first one without a space between them. Mature waves are generated in an environment where small amount of X and A are left in the abundant N field. (Recall the initial condition that only X particles are planted at the center in the uniformly distributed N and A.) In this environment, such a small amount of A cannot be used to activate all the existing X quickly and consequently the product X soon generates I, which ignites subprocess (S) again. In summary, the residual X and A remaining after incomplete consumption works as seeds that keep the system oscillatory between the subprocesses (P) and (S) such that (P) → (S) → (P) → (S) → ⋯.

B. Mechanism of the other spatiotemporal patterns

On the basis of the detailed mechanism of wave propagation studied above for the CRP, we here summarize the generating mechanisms of the other spatiotemporal patterns.

1. RRP [Fig. 2(a)]

RRP are generated in case where the initial quantity of activator A (A_0) is relatively small. In this case, the mature

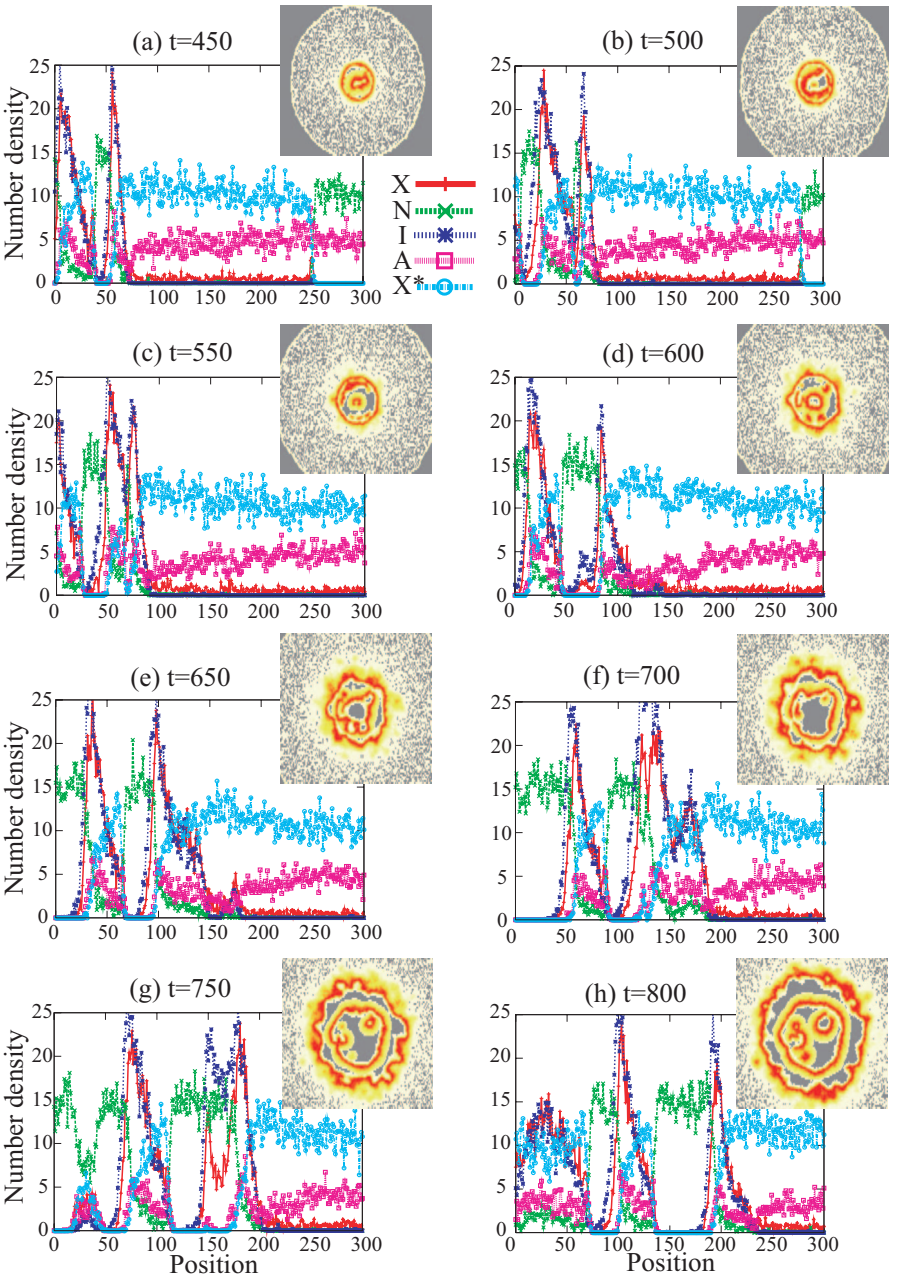

FIG. 8. (Color) Propagation of the second and third waves, which are merged to a single wave.

waves are less frequently generated one after another. This is because the second wave is quickly propagated, proceed, and leave. As a result, just as described above, the residual agents X and A can have some induction time to encounter each other to react as $X+A \rightarrow X^*$ to form a new core. Thus the new cores can be generated here and there rather randomly, from which new waves emerge.

Furthermore, it is helpful to recall that the initial distribution of X is a pointlike one at the center of the system, and N and A are uniformly distributed over the system. No I is initially prepared. If the concentration of A_0 is low, the reactions of subprocess (P), Eqs. (4a) and (4b), should be over quickly, and therefore the second wave can be generated in the earlier stage. On the other hand, A is eventually transformed to X^* and/or N in a periodic manner subject to the conservation of $N+A+X^*$. Therefore the smaller amount of A_0 gives rise to the less X^* and/or N within the mature waves in subprocesses (P) and (S). Thus, the firing of subprocess (P) is less probable and the core generation is retarded.

2. TWP [Fig. 2(c)]

In contrast to RRP, TWP is generated in case where A_0 is large. For the opposite reason to that for the RRP formation, many mature waves are formed one after another frequently and collide each other. Thus numerous spiral waves are distributed in a random fashion, which are densely packed in a slowly expanding circle of the second wave. Depending on the timing of the formation and passage of the second wave, CRP is generated and then TWP can follow it as seen in Fig. 2(c).

3. SHD

In case where A_0 is excessively prepared over the amount of N, the distributions of X, X^*, and A become uniform over

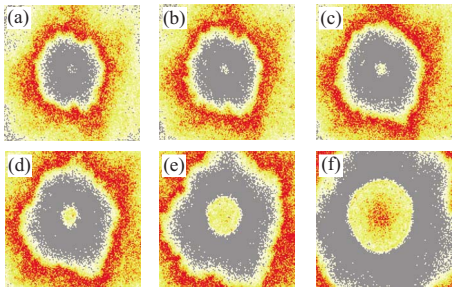

FIG. 9. (Color online) A very small amount of X and A (or X^*) left in the central spot due to the stochastic fluctuation realized by the CA dynamics ignites the next reaction process. Once this happens, the small wave is amplified and propagated in the macroscopic scale since the field is already full of N. (a) $t=300$, (b) $t=312$, (c) $t=324$, (d) $t=336$, (e) $t=360$, and (f) $t=400$.

the system after exhausting both N and I. This final distribution corresponds to that in the region between the first and the second waves (see Fig. 7). In this case, only the first wave emerges from the pointlike distribution of X at the center, but N in the center region is too much exhausted to generate the second wave. This is because X produced by the autocatalytic reaction in subprocess (P) immediately reacts with A in the center region because of excess A and changes to X^* [reaction (2a)]. Thus X cannot increase and consequently I does not increase either. This implies that there is no supply of new N after the original N has been consumed up. After all, the entire reaction system is frozen without generating the second wave.

4. VP

In case where N is overwhelmingly prepared over A initially, all the X disappear from the system. In this case, the second wave travels with a speed a little faster than that of the first wave. They eventually collide, and virtually no core, from which new waves can generate, is created, since the field falls into a fixed point where only N exists.

IV. EXCITABLE WAVES SUCCESSIVELY GENERATED BY INTERNAL STOCHASTICITY

We have observed above that even after the subprocesses (S) is effectively over, a small amount of X and A (or X^*)

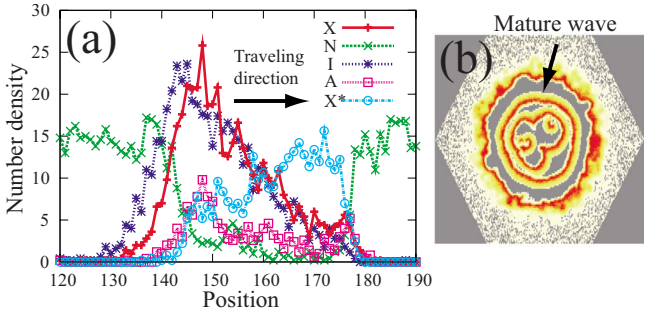

FIG. 10. (Color online) (a) The distributions of the individual components near the first mature wave in the radial direction at $t=900$. (b) The snapshot of X distribution.

TABLE II. System parameters chosen for the reaction-diffusion equations.

x_0	1.0	D_X	0.2	k_1	3.0
n_0	10.0	D_N	0.2	k_1^*	1.0
i_0	0.0	D_I	0.2	k_2	3.0
a_0	10.0	D_A	0.2	k_3	2.0
x_0^*	0.0	D_{X^*}	0.2	k_4	4.0
				k_5	3.0

remaining unburned can ignite the subprocess (P) in the field of rich N. That is, the incomplete burning of X and A, or imperfect burning of subprocess (S) due to the inherent stochastic nature of CA is responsible for the successive formation of excitable waves. To establish this mechanism in more general theoretical context, we resume our study with the notion of excitable system, which is of a different kind from the FitzHugh-Nagumo (FN). In doing so, we borrow the help of the reaction-diffusion equation method (RD) with and without noise.

A. Excitable system supported by a hidden oscillation and diffusion

1. Stable fixed point and its induced instability

First of all, we note that the present system, which hides oscillation behind between the subprocesses (P) and (S), has actually a very clear and trivial stable fixed point, that is, $d[X]/dt=d[N]/dt=d[A]/dt=d[X^*]/dt=d[I]/dt=0$ at $[X]=[X^*]=[I]=0$. Thus, this entire system in the mean field is not expected to undergo self-sustained temporal oscillation. However, to understand more about the physical significance of the stable fixed point and its property, we explore the dynamics with use of the RD equations, representing the rate process of the model [Eqs. (2a)–(2e)] as

$$\frac{\partial x}{\partial t} = -k_1 x a + k_1^* x^* + 2k_2 x^* n - k_3 x + D_X \nabla^2 x, \tag{7a}$$

$$\frac{\partial n}{\partial t} = -k_2 x^* n + k_4 a i + D_N \nabla^2 n, \tag{7b}$$

$$\frac{\partial i}{\partial t} = 3k_3 x - k_4 a i - k_5 i + D_I \nabla^2 i, \tag{7c}$$

$$\frac{\partial a}{\partial t} = -k_1 x a + k_1^* x^* + 2k_2 x^* n - k_4 a i + D_A \nabla^2 a, \tag{7d}$$

$$\frac{\partial x^*}{\partial t} = k_1 x a - k_1^* x^* - k_2 x^* n + D_{X^*} \nabla^2 x^*, \tag{7e}$$

where $x(\mathbf{z},t), n(\mathbf{z},t), i(\mathbf{z},t), a(\mathbf{z},t)$, and $x^*(\mathbf{z},t)$ are the spatiotemporal concentration of X, N, I, A, and X^*, respectively, in the two-dimensional space $\mathbf{z}$ and time t. k_1 and k_1^* are the rate constants of the forward and reverse reaction process (2a), and k_2, k_3, k_4, and k_5 are the rate constants of reactions

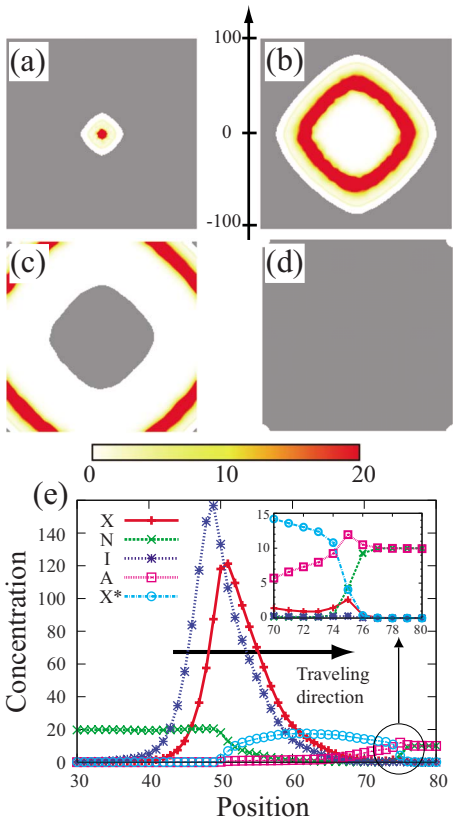

FIG. 11. (Color online) [(a)–(d)] Single excitable wave in the RD equations (7a)–(7e). (a) $t=2.5$, (b) $t=15.0$, (c) $t=30.0$, and (d) $t=50.0$. After the single passage of a pulse wave, the field gets filled with N only. (e) The concentration of each component changes in the manner similar to those in Fig. 10(a). The inset shows a magnification of the part surrounded by the large circle.

(2b)–(2e), respectively. D_j is the diffusion constant of the component j. No external noise is introduced. Table II lists the system parameters for the present RD equations. We solve the above RD Eqs. (7a)–(7e) using the Crank-Nicolson scheme [21] on a square grid to obtain the global solutions of $x(\mathbf{z},t), n(\mathbf{z},t), i(\mathbf{z},t), a(\mathbf{z},t)$, and $x^*(\mathbf{z},t)$. An obvious fixed point of this set of differential equations is found at $x(\mathbf{z},t)=0$, $i(\mathbf{z},t)=0$, $x^*(\mathbf{z},t)=0$, $n(\mathbf{z},t)=$an arbitrary constant, $a(\mathbf{z},t)=$an arbitrary constant. Therefore the choice of $x(\mathbf{z},0)=0$, $i(\mathbf{z},0)=0$, $x^*(\mathbf{z},0)=0$ and the uniform distribution of $n(\mathbf{z},0)$ and $a(\mathbf{z},0)$ makes sense as a stable initial condition. At the same time, it is expected that the asymptotic solution at a large t may fall into the manifold of these fixed points.

The most striking observation in the above RD calculations is that only a transient symmetric ring wave is generated, which disappears shortly, and no long-standing spatiotemporal pattern occurs in marked contrast to the CA solutions. Figures 11(a)–11(d) show such a space-time propagation of the excitable wave of a ring shape. In panel (d) at $t=50.0$, the field is occupied by N only. Panel (e) displays a snapshot of the spatial distribution of the individual component in the RD. Two peaks of X in the wave front are observed; one is a small bump at $r\sim 75$ and the other is the higher peak at $r\sim 50$. They are similar to the first and second waves in the CA, respectively.

Thus it is concluded that the stable fixed point, $[X]=[X^*]=[I]=0$, is stable within its own closed space, but it turns to be unstable, once a tiny droplet containing X and A is added from the outside of the system. We may say that this fixed point is "stable internally but unstable externally." What is more, the induced instability thus brought in becomes quickly amplified to a macroscopic level due to the autocatalytic proliferation reaction.

2. Response to a weak external noise: A difference from the FN excitation

The above property of the "stable" fixed point leads to a significantly different behavior of excitation from that of the FN model in the response to external noise. The FN sits at the stable fixed point and can be excited by external noise (perturbation), which is larger than a threshold value. Usually this threshold should not be very small. This is because if a neural connection is easily excited even by a very weak noise, or in other words, if it is unstable to any weak noise, it should be always kept fired almost continuously.

On the other hand, system PIA is unstable to adding a tiny droplet of containing X and A, and therefore, it is expected to be also unstable to external noise that can induce a weak fluctuation of the concentration of the component. To confirm this expectation, we numerically study the present dynamics in terms of the RD equations, to which an external noise is added as

$$\frac{\partial x}{\partial t} = -k_1 xa + k_1^* x^* + 2k_2 x^* n - k_3 x + D_X \nabla^2 x + \eta_a \xi_a(\mathbf{z},t), \tag{8a}$$

$$\frac{\partial n}{\partial t} = -k_2 x^* n + k_4 ai + D_N \nabla^2 n, \tag{8b}$$

$$\frac{\partial i}{\partial t} = 3k_3 x - k_4 ai - k_5 i + D_I \nabla^2 i, \tag{8c}$$

$$\frac{\partial a}{\partial t} = -k_1 xa + k_1^* x^* + 2k_2 x^* n - k_4 ai + D_A \nabla^2 a + \eta_b \xi_b(\mathbf{z},t), \tag{8d}$$

$$\frac{\partial x^*}{\partial t} = k_1 xa - k_1^* x^* - k_2 x^* n + D_{X^*} \nabla^2 x^*, \tag{8e}$$

where $\xi_a(\mathbf{z},t)$ and $\xi_b(\mathbf{z},t)$ are the Gaussian white noises, and η_a and η_b are the amplitudes of the fluctuation.

Our numerical realization of the above equations shows very clearly that a small amount of X and A produced artificially by the external fluctuation form a new core of the next wave in the abundant N field, and they generate the successive propagation of the circular waves starting from the randomly formed cores. Figure 12 displays the time series of such propagation under the parameters $\eta_a=\eta_b=0.5$: since X is produced by the external fluctuation, X immediately proliferates everywhere before the initially planted core expands [(a) $t=2.0$, (b) $t=3.5$], and then X is eventually extinguished

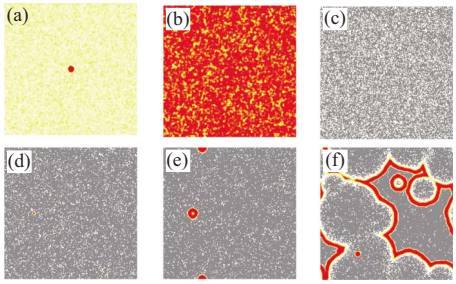

FIG. 12. (Color online) Generation of successive waves in the RD Eqs. (8a)–(8e) subject to an external noise of $\eta_a=\eta_b=0.5$. (a) $t=2.0$, (b) $t=3.5$, (c) $t=10.0$, (d) $t=16.0$, (e) $t=20.0$, and (f) $t=50.0$. See the text about the description of the varying field.

leaving a large amount of N [(c) $t=10.0$]. However, a small amount of X and A produced artificially by the external fluctuation generates a new core of the next wave [(d) $t=16.0$], and it propagates in the abundant N field [(e) $t=20.0$]. Thus, artificially planted X and A by the external fluctuation leads to the successive propagation of the circular waves starting from the randomly formed cores [(f) $t=50.0$].

B. Driving the excitable system with internal stochasticity and diffusion

Although even a weak external noise can cause successive generation and propagation of the excitable waves in RD, it is quite obvious that the external noise is not the physical origin of the concentric ring pattern and the others observed in CA dynamics of Secs. II and III. One reason for this conclusion is that the present CA does not include any external noise throughout the calculations, and another one is that the excitable waves observed above in the RD equations with external noise disappear quickly as soon as the external noise is switched off.

1. Internal stochasticity

The dramatic difference of the pattern formation in RD from that of the CA as studied in the preceding subsection is readily understood by confirming that all the components, X, X^*, I, and A except for N, have been burned out completely within its (single) wave front, and concomitantly nothing other than N is left behind after the passage of the wave (there is no stochastic factor for a small amount of these components to be unburned in the RD scheme). [Recall Figs. 11(a)–11(d)] This directly implies that there remains neither X, A nor X^* that is required to form a new core of the next wave (see Fig. 9). Thus, the field has fallen into the stable fixed point that represents a state filled with only N. To reproduce the successive waves in the RD, therefore, one needs to keep adding such a seed one after another, and this is indeed the case.

In the CA dynamics, on the other hand, some of the residual (unburned) elements of X and A are carried by diffusion in a stochastic manner and may encounter each other with the help of diffusion. By the collision, the next process [subprocess (P)] is fired and the wave is amplified quickly to the macroscopic level. These residual elements remain due to the stochastic fluctuation dynamics inherent to CA.

To survey the role of the intrinsic stochastic fluctuation in the CA dynamics for generating successive wave propagation more clearly, we next introduce the augmented RD equations which include threshold dynamics with local fluctuation (more details in Ref. [17]). We try to mimic the stochastic fluctuation of CA by regarding it as internal fluctuation (not an external noise). There can be many ways to do so. Indeed we have tested several of them and found not much difference among them. Below is one such realization.

$$\frac{\partial x}{\partial t} = -[k_1 x_\varepsilon a_\varepsilon + \eta_1 \xi_1(\mathbf{z},t)] + [k_1^* x_\varepsilon^* + \eta_1^* \xi_1^*(\mathbf{z},t)] + [2k_2 x_\varepsilon^* n_\varepsilon + 2\eta_2 \xi_2(\mathbf{z},t)] - [k_3 x_\varepsilon + \eta_3 \xi_3(\mathbf{z},t)] + D_X \nabla^2 x, \tag{9a}$$

$$\frac{\partial n}{\partial t} = -[k_2 x_\varepsilon^* n_\varepsilon + \eta_2 \xi_2(\mathbf{z},t)] + [k_4 a_\varepsilon i_\varepsilon + \eta_4 \xi_4(\mathbf{z},t)] + D_N \nabla^2 n, \tag{9b}$$

$$\frac{\partial i}{\partial t} = [3k_3 x_\varepsilon + 3\eta_3 \xi_3(\mathbf{z},t)] - [k_4 a_\varepsilon i_\varepsilon + \eta_4 \xi_4(\mathbf{z},t)] - [k_5 i_\varepsilon + \eta_5 \xi_5(\mathbf{z},t)] + D_I \nabla^2 i, \tag{9c}$$

$$\frac{\partial a}{\partial t} = -[k_1 x_\varepsilon a_\varepsilon + \eta_1 \xi_1(\mathbf{z},t)] + [k_1^* x_\varepsilon^* + \eta_1^* \xi_1^*(\mathbf{z},t)] + [2k_2 x_\varepsilon^* n_\varepsilon + 2\eta_2 \xi_2(\mathbf{z},t)] - [k_4 a_\varepsilon i_\varepsilon + \eta_4 \xi_4(\mathbf{z},t)] + D_A \nabla^2 a, \tag{9d}$$

$$\frac{\partial x^*}{\partial t} = [k_1 x_\varepsilon a_\varepsilon + \eta_1 \xi_1(\mathbf{z},t)] - [k_1^* x_\varepsilon^* + \eta_1^* \xi_1^*(\mathbf{z},t)] - [k_2 x_\varepsilon^* n_\varepsilon + \eta_2 \xi_2(\mathbf{z},t)] + D_{X^*} \nabla^2 x^*, \tag{9e}$$

where x_ε, n_ε, i_ε, a_ε, and x_ε^* are the quasidiscrete concentration of X, N, I, A, and X^*, respectively. Here, x_ε is defined as

$$x_\varepsilon \equiv \begin{cases} x & (x \geq \varepsilon) \\ 0 & (x < \varepsilon), \end{cases} \tag{10}$$

by using the threshold value ε. n_ε, i_ε, a_ε, and x_ε^* are defined in a similar manner. $\xi_1(\mathbf{z},t)$, $\xi_1^*(\mathbf{z},t)$, $\xi_2(\mathbf{z},t)$, $\xi_3(\mathbf{z},t)$, $\xi_4(\mathbf{z},t)$, and $\xi_5(\mathbf{z},t)$ are the Gaussian white noises. The discretization as done in Eq. (10) has been considered to mimic the finite process inherent in CA. The amplitude of the fluctuation in a reaction i, η_i, can be estimated at the square root of the mean production rate in the reaction i; $\eta_1=\sqrt{k_1 x_\varepsilon a_\varepsilon \varepsilon}$, $\eta_1^*=\sqrt{k_1^* x_\varepsilon^* \varepsilon}$, $\eta_2=\sqrt{k_2 x_\varepsilon^* n_\varepsilon \varepsilon}$, $\eta_3=\sqrt{k_3 x_\varepsilon \varepsilon}$, $\eta_4=\sqrt{k_4 a_\varepsilon i_\varepsilon \varepsilon}$, and $\eta_5=\sqrt{k_5 i_\varepsilon \varepsilon}$. We set the same system parameters as the noiseless RD Eqs. (7a)–(7e) listed in Table II. As shown in Fig. 13, these equations can successfully generate the successive wave propagation that is similar to those observed in the CA dynamics. A propagating wave leaves behind tiny residues of X [panel (b)], and then it forms the next wave [panel (c)]. Gradually, several cores of the new waves are formed [panel (d)], and finally the steady successive wave propagation fills the entire

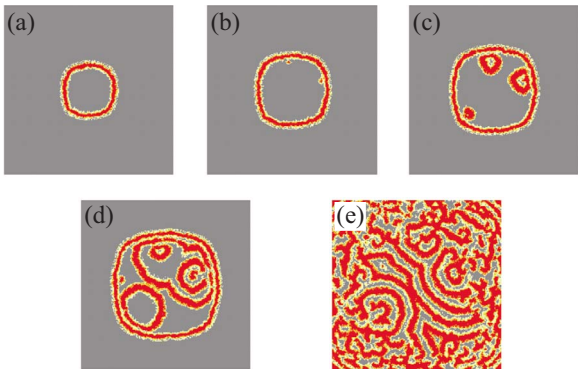

FIG. 13. (Color online) Generation of successive wave in the RD Eqs. (9a)–(9e). A propagating wave leaves the tiny residues of X behind [(a) $t=25$, (b) $t=34$], which form the next waves [(c) $t=40$]. Gradually, several cores are formed [(d) $t=50$] and eventually the successive waves fill the entire field [(e) $t=100$].

field with traveling waves [panel (e)]. However, it should be noted that the "internal fluctuation" thus incorporated cannot be rigorously distinguished from the "external noise" in their effects on computation. After all, what we could confirm is only that to reproduce the results of CA in terms of the RD equations one needs appropriate noise anyway, either external or internal.

Incidentally, we would like to mention to the mean-field dynamics of the above Eqs. (9a)–(9e), from which we have intentionally removed the diffusion terms to see the role of diffusion. There are two important roles played by diffusion. One is of course the driving force to propagate an excitable wave outward. The second is that it assists the residual unburned elements in the stochastic process to encounter leading to form a core of another excitation. Therefore, as expected, the RD with internal fluctuation but without diffusion shows only a single excitation (pulse generation) that does not propagate in space. Thus it turns out that both the inherent stochastic fluctuation and the diffusion are important to generate the successive wave propagation.

2. Stochastic versus deterministic methods to solve dynamical equations

As clarified above, the self-sustained oscillation in CA dynamics to generate and propagate the concentric ring waves is due to the stochastic fluctuation leaving a small amount of unburned components such as X and A. This fluctuation is repeated whenever such an excitable wave is propagated. As shown above, on the other hand, the deterministic RD equations without any noise or internal fluctuation give only the solutions of burning the components completely and thereby leaving only N behind, which does not reproduce a self-sustained oscillation.

In studying dynamical systems in general, one can usually choose either the deterministic approach based on differential equations or the stochastic method basically resorting to "random walk." In the latter methods, discrete variables are often adopted and global symmetry is missing in the local solutions. In linear dynamics such as the simple diffusion equation and the Schrödinger wave equation, it is mathematically proved that the perfect integration (summation) of the path solutions based on random walks gives a global distribution function of the differential equations [22]. In nonlinear regime, Gillespie [23] argued that the stochastic approach has a firmer physical basis and hence proposed his Monte Carlo based algorithm to treat homogeneous chemical systems. (See also the work of Gibson and Bruck [24].) The naive RD is a typical example of the deterministic approach, while CA [16] and Monte Carlo based methods such as the Gillespie method along with their extensions are well known as the stochastic method. Despite the claim of Gillespie [23] that the stochastic method is physically more preferable, it is generally assumed that the difference between the solutions of the deterministic and stochastic methods is small enough to the order of stochastic fluctuation. However, the present work has found that it is not necessarily the case. We here have reported a generic example of very large discrepancy (qualitatively difference) between the deterministic RD solutions and the stochastic counterparts.

V. CONCLUDING REMARKS

We have studied a nonlinear system that contains an activation process in autocatalytic proliferation dynamics along with the process of its self-suppression. The model turns out to generate various spatiotemporal patterns with the cellular automaton method. We have studied the mechanism of these pattern formations. In particular, it has been shown that the geometry and timing of the first, second, and mature waves are critical to generate these patterns. It turns out that the ratio of the activator and nutrition in the initial condition is a key parameter to determine the patterns. Therefore, the spatial gradient of the initial distribution of the activator can be used as a parameter that may lead to the production of interesting dynamical patterns. Eventually this procedure will make it possible to control the pattern formation.

We have also analyzed the mechanism of successive generation of propagating excitable waves in terms of the difference between RD and CA. First of all, the present system is an excitable system having a stable fixed point, which turns out to be unstable to adding a small amount of a couple of components from the outside. This excitation mechanism is therefore different from that represented by the FN system. For the present system to be an excitable one, the following three factors have been found to play key roles: (1) the reaction network is composed of two subprocesses, which can potentially induce temporary oscillation by the stochastic internal fluctuation. Even a very small fluctuation can be amplified to a macroscopic level due to the proliferation dynamics lying behind. However, the system falls into a stable fixed point unless the following two mechanisms work out. (2) After a single circuit of reactions is over, in which a pulse wave is propagated outward, a few particles can remain unburned in the field in a stochastic manner. (3) These unburned elements collide with each other with the help of diffusion and ignite the next reaction step, eventually leading to another wave of macroscopic size. The CA naturally materializes this stochastic process of incomplete reaction, but RD without noise does not. Indeed RD without noise pro-

duces only a single pulse wave but does not give birth to the successive excitable waves, and in fact RD with noise can generate the successive wave propagation.

In short, a tiny stochastic fluctuation is amplified to a macroscopic level as a pulse wave due to proliferation dynamics, and this process can be repeated many times giving successive waves, the repetition of which is actually supported by an implicit mechanism of temporal oscillation between activation and its self-suppression.

ACKNOWLEDGMENTS

This work was supported in part by the Grant-in-aid for Basic Science from the Ministry of Education, Culture, Sports, Science and Technology of Japan. One of the authors (K.O.) was financially supported by the JSPS.

APPENDIX: ALGORITHM FOR REACTION PROCESSES

We here introduce three characteristic features of the CA rules that are difficult for the ordinary rate equation method to describe.

(1) There are two elementary reaction processes consuming A in the model [Eqs. (2a)–(2e)]; activation reaction for the proliferation Eq. (2a) and inhibitory reaction Eq. (2d). There is no *a priori* reason to determine the order of choosing the elementary processes. So, one of these reactions is stochastically selected depending on the number of particles related to them (X or I) at the same node. Then, we determine whether selected reaction actually takes place or not, with a predetermined reaction probability.

(2) Consider the decomposition reaction of X as in Eq. (2c). Basically, its rate should depend only on the number of X at each node. However, since X can be involved in the other reaction Eq. (2a) at the same time, the decomposition reaction cannot be treated independently as though no other reactions existed. Thus, the decomposition reaction of X effectively depends on the local circumstances. Similarly, the decomposition of I also effectively depends on the local circumstances.

(3) We make a rule that in proliferation reaction, one of newly born $X's$ should be recoiled and thereby pushed out from the node at which they were born with a probability s predetermined. This effect is described as follows. When X splits into two particles by the proliferation reaction, one of them is stochastically forced to push out to a neighboring node.

In this appendix, we describe the CA rules in a great detail. In what follows, X_i^z denotes the number of X particles at a node z before a reaction, $\Delta X_+^z(\Delta X_-^z)$ indicate the increment (decrement) of the number of X particles at the node z during the reaction, whereas X_f^z denotes the number of X particles at the node z after the reaction, satisfying $X_f^z=X_i^z+\Delta X_+^z-\Delta X_-^z$. For the other components, the similar notations are used.

1. Treatment of push-out effect

When a single X particle splits into two, one of them can be stochastically pushed out to a neighboring node or remains at the original point. We here define s as a probability for the X particle to stay at the original node ($0\leq s\leq 1$). Also, since the particle is pushed out to isotropic directions, the probability to be pushed out to one of the nearest-neighbor nodes is $\frac{1-s}{6}$. In this paper, we set $s=0.99$ throughout. A random number R in $[0,1)$ is used to determine a node to which one of two split X particles should move. We denote these nodes as S.

2. CA rules

(1) Perform the following steps from step (2) to step (7) for all the nodes.
(2) Calculate the probability p_c^z to choose the reaction processes [activation Eq. (2a) or inhibition Eq. (2d)] depending on the local state (X_i^z and I_i^z) at a node z, $p_c^z=\frac{\tanh(X_i^z-I_i^z)+1}{2}$ [25].
(3) Repeat the next substeps A_i^z times at the node z.
  (a) Generate a random number R in $[0,1)$.
  (b) If $R<p_c^z$, then perform the next substeps:
    (i) Go to the procedure A.
    (ii) If the procedure A returns "true," then go back to step (3).
    (iii) Go to the procedure D. Then, go back to step (3).
  (c) If $R\geq p_c^z$, then perform the next substeps:
    (i) Go to the procedure D.
    (ii) If the procedure D returns "true," then go back to step (3).
    (iii) Go to the procedure A. Then, go back to step (3).
(4) Repeat the procedure C ($X_i^z-\Delta X_-^z$) times at the node z.
(5) Repeat the next substeps X_i^{*z} times at the node z.
  (a) Go to the procedure B.
  (b) If the procedure B returns "true," then go back to step (5).
  (c) Go to the procedure F. Then, go back to step (5).
(6) Repeat the procedure E ($I_i^z-\Delta I_-^z$) times at the node z.
(7) Go back to step (2).
(8) After the above procedures are completed, calculate X_f^z, N_f^z, I_f^z, A_f^z, and X_f^{*z} for all the nodes.

3. Reaction procedures

A: $X+A\rightarrow X^*$ [Eq. (2a) forward].
  (a) If $X_i^z-\Delta X_-^z\neq 0$, then perform the next steps (b) and (c). Otherwise, return "false" [Eq. (2a) forward does not occur] and go back to the calling step without change.
  (b) Generate a random number R in $[0,1)$.
  (c) If $R<r_1$, then add unity to ΔX_-^z, ΔA_-^z, and ΔX_+^{*z}, respectively, and then return "true" [Eq. (2a) forward occurs] and go back to the calling step. Otherwise, return "false" and go back to the calling step without change.
B: $X^*+N\rightarrow 2X+2A$ [Eq. (2b)].
  (a) If $N_i^z-\Delta N_-^z\neq 0$, then perform the next steps (b) and (c). Otherwise, return "false" [Eq. (2b) does

not occur] and go back to the calling step without change.
(b) Generate a random number R in $[0,1)$.
(c) If $R<r_2$, then add unity to ΔX_-^{*z}, ΔN_-^z, ΔX_+^S, and ΔX_+^z, respectively, and add 2 to ΔA_+^z, and then return "true"[Eq. (2b) occurs] and go back to the calling step. Otherwise, return "false" and go back to the calling step without change.

C: $X \rightarrow P_1 + \alpha I$ [Eq. (2c)].
(a) Generate a random number R in $[0,1)$.
(b) If $R<r_3$, then add unity to ΔX_-^z, and add α to ΔI_+^z [Eq. (2c) occurs].
(c) Go back to the calling step.

D: $A+I \rightarrow N$ [Eq. (2d)].
(a) If $I_i^z - \Delta I_-^z \neq 0$, then perform the next steps (b) and (c). Otherwise, return "false" [Eq. (2d) does not occur] and go back to the calling step without change.
(b) Generate a random number R in $[0,1)$.
(c) If $R<r_4$, then add unity to ΔA_-^z, ΔI_-^z, and ΔN_+^z, respectively, and then return "true" [Eq. (2d) occurs] and go back to the calling step. Otherwise, return "false" and go back to the calling step without change.

E: $I \rightarrow P_2$ [Eq. (2e)].
(a) Generate a random number R in $[0,1)$.
(b) If $R<r_5$, then add unity to ΔI_-^z [Eq. (2e) occurs].
(c) Go back to the calling step.

F: $X+A \leftarrow X^*$ [Eq. (2a) backward].
(a) Generate a random number R in $[0,1)$.
(b) If $R<r_1^*$, then add unity to ΔX_-^{*z}, ΔX_+^z, and ΔA_+^z, respectively [Eq. (2a) backward occurs].
(c) Go back to the calling step.

[1] C. Sachs, M. Hildebrand, S. Völkening, J. Wintterlin, and G. Ertl, Science **293**, 1635 (2001); M. Nagasaka, H. Kondoh, and T. Ohta, J. Chem. Phys. **122**, 204704 (2005).
[2] J. D. Murray, Sci. Am. **258**, 80 (1988); S. Kondo and R. Asai, Nature (London) **376**, 765 (1995).
[3] R. Imbihl and G. Ertl, Chem. Rev. **95**, 697 (1995).
[4] J. Lechleiter, S. Girard, E. Peralta, and D. Clapham, Science **252**, 123 (1991).
[5] J. J. Tyson, K. A. Alexander, V. S. Manoranjaan, and J. D. Murray, Physica D **34**, 193 (1989).
[6] N. A. Gorelova and J. Bures, J. Nurobiol. **14**, 353 (1983).
[7] J. M. Davidenko, A. V. Pertsov, R. Salomonsz, W. Baxter, and J. Jalife, Nature (London) **355**, 349 (1992).
[8] R. J. Field, E. Kőrös, and R. M. Noyes, J. Am. Chem. Soc. **94**, 8649 (1972).
[9] R. J. Field and R. M. Noyes, J. Chem. Phys. **60**, 1877 (1974).
[10] J. P. Keener and J. J. Tyson, Physica D **21**, 307 (1986).
[11] Y. Kuramoto, *Chemical Oscillations, Waves, and Turbulence* (Springer-Verlag, Berlin, 1984).
[12] R. Kapral and K. Showalter, *Chemical Waves and Patterns* (Kluwer, Dordrecht, 1995).
[13] B. Lindner, J. García-Ojalvo, A. Neiman, and L. Schimansky-Geier, Phys. Rep. **392**, 321 (2004).
[14] A. S. Pikovsky and J. Kurths, Phys. Rev. Lett. **78**, 775 (1997).
[15] J. García-Ojalvo and J. M. Sancho, *Noise in Spatially Extended Systems* (Springer, New York, 1999).
[16] B. Chopard and M. Droz, *Cellular Automata Modeling of Physical Systems* (Cambridge University Press, Cambridge, England, 1998).
[17] K. Odagiri and K. Takatsuka, Phys. Rev. E **79**, 026202 (2009).
[18] S. Yaguma, K. Odagiri, and K. Takatsuka, Physica D **197**, 34 (2004).
[19] L. G. Morelli and D. H. Zanette, Phys. Rev. E **58**, R8 (1998); P. Grassberger, *ibid.* **59**, R2520 (1999).
[20] T. Ariizumi, N. Moriya, H. Uchiyama, and M. Asashima, Rouxs Arch. Dev. Biol. **200**, 230 (1991).
[21] W. H. Press, S. A. Teukolsky, W. T. Vetterling, and B. P. Flannery, *Numerical Recipes in C*, 2nd ed. (Cambridge University Press, Cambridge, England, 2002).
[22] L. S. Schulman, *Techniques and Applications of Path Integration* (Wiley, New York, 1981).
[23] D. T. Gillespie, J. Chem. Phys. **81**, 2340 (1977).
[24] M. A. Gibson and J. Bruck, J. Phys. Chem. A **104**, 1876 (2000).
[25] We use tanh-function for more sensitive switching between the self-replication and the inhibition according to the local state. Even if we use $p_c^z = \frac{X_i^z}{X_i^z + F_i^z}$ as the choice probability p_c^z, system PIA can generate spatiotemporal patterns, although these patterns have rather vague boundaries.